Geophysical Monograph 57
IUGG Volume 8

Evolution of Mid Ocean Ridges

John M. Sinton
Editor

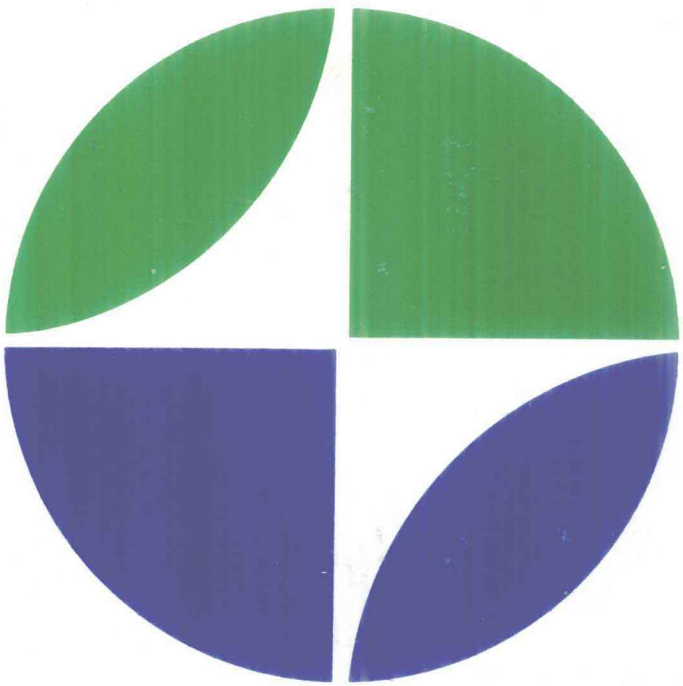

Geophysical Monograph 57
IUGG Volume 8

Evolution of Mid Ocean Ridges

John M. Sinton, Editor

American Geophysical Union
International Union of Geodesy and Geophysics

Geophysical Monograph/IUGG Series

Library of Congress Cataloging-in-Publication Data

Evolution of mid-ocean ridges.

(Geophysical monograph ; 57) (IUGG ; v. 8)
Based on IUGG Union Symposium 9 held during the 1987 IUGG General Assembly at Vancouver, Canada, and jointly sponsored by IAVCEI and others.
1. Sea—floor spreading—Congresses. 2. Mid-ocean ridges—Congresses. I. Sinton, John M. II. IUGG Union Symposium (9 : 1987 : Vancouver. B.C.) III. International Association of Vocanology and Chemistry of the Earth's Interior. IV. Series. V. Series: IUGG (Series) ; v. 8.
QE511.7.E96 1989 551.46'08 89-18531
ISBN 0-87590-458-0

Printed in the United States of America.

GEOPHYSICAL MONOGRAPH SERIES

Geophysical Monograph Volumes

1 **Antarctica in the International Geophysical Year** *A. P. Crary, L. M. Gould, E. O. Hulburt, Hugh Odishaw, and Waldo E. Smith (Eds.)*
2 **Geophysics and the IGY** *Hugh Odishaw and Stanley Ruttenberg (Eds.)*
3 **Atmospheric Chemistry of Chlorine and Sulfur Compounds** *James P. Lodge, Jr. (Ed.)*
4 **Contemporary Geodesy** *Charles A. Whitten and Kenneth H. Drummond (Eds.)*
5 **Physics of Precipitation** *Helmut Weickmann (Ed.)*
6 **The Crust of the Pacific Basin** *Gordon A. Macdonald and Hisahi Kuno (Eds.)*
7 **Antarctica Research: The Matthew Fontaine Maury Memorial Symposium** *H. Wexler, M. J. Rubin, and J. E. Caskey, Jr. (Eds.)*
8 **Terrestrial Heat Flow** *William H. K. Lee (Ed.)*
9 **Gravity Anomalies: Unsurveyed Areas** *Hyman Orlin (Ed.)*
10 **The Earth Beneath the Continents: A Volume of Geophysical Studies in Honor of Merle A. Tuve** *John S. Steinhart and T. Jefferson Smith (Eds.)*
11 **Isotope Techniques in the Hydrologic Cycle** *Glenn E. Stout (Ed.)*
12 **The Crust and Upper Mantle of the Pacific Area** *Leon Knopoff, Charles L. Drake, and Pembroke J. Hart (Eds.)*
13 **The Earth's Crust and Upper Mantle** *Pembroke J. Hart (Ed.)*
14 **The Structure and Physical Properties of the Earth's Crust** *John G. Heacock (Ed.)*
15 **The Use of Artificial Satellites for Geodesy** *Soren W. Henricksen, Armando Mancini, and Bernard H. Chovitz (Eds.)*
16 **Flow and Fracture of Rocks** *H. C. Heard, I. Y. Borg, N. L. Carter, and C. B. Raleigh (Eds.)*
17 **Man-Made Lakes: Their Problems and Environmental Effects** *William C. Ackermann, Gilbert F. White, and E. B. Worthington (Eds.)*
18 **The Upper Atmosphere in Motion: A Selection of Papers With Annotation** *C. O. Hines and Colleagues*
19 **The Geophysics of the Pacific Ocean Basin and Its Margin: A Volume in Honor of George P. Woollard** *George H. Sutton, Murli H. Manghnani, and Ralph Moberly (Eds.)*
20 **The Earth's Crust: Its Nature and Physical Properties** *John G. Heacock (Ed.)*
21 **Quantitative Modeling of Magnetospheric Processes** *W. P. Olson (Ed.)*
22 **Derivation, Meaning, and Use of Geomagnetic Indices** *P. N. Mayaud*
23 **The Tectonic and Geologic Evolution of Southeast Asian Seas and Islands** *Dennis E. Hayes (Ed.)*
24 **Mechanical Behavior of Crustal Rocks: The Handin Volume** *N. L. Carter, M. Friedman, J. M. Logan, and D. W. Stearns (Eds.)*
25 **Physics of Auroral Arc Formation** *S.-I. Akasofu and J. R. Kan (Eds.)*
26 **Heterogeneous Atmospheric Chemistry** *David R. Schryer (Ed.)*
27 **The Tectonic and Geologic Evolution of Southeast Asian Seas and Islands: Part 2** *Dennis E. Hayes (Ed.)*
28 **Magnetospheric Currents** *Thomas A. Potemra (Ed.)*
29 **Climate Processes and Climate Sensitivity (Maurice Ewing Volume 5)** *James E. Hansen and Taro Takahashi (Eds.)*
30 **Magnetic Reconnection in Space and Laboratory Plasmas** *Edward W. Hones, Jr. (Ed.)*
31 **Point Defects in Minerals (Mineral Physics Volume 1)** *Robert N. Schock (Ed.)*
32 **The Carbon Cycle and Atmospheric CO_2: Natural Variations Archean to Present** *E. T. Sundquist and W. S. Broecker (Eds.)*
33 **Greenland Ice Core: Geophysics, Geochemistry, and the Environment** *C. C. Langway, Jr., H. Oeschger, and W. Dansgaard (Eds.).*
34 **Collisionless Shocks in the Heliosphere: A Tutorial Review** *Robert G. Stone and Bruce T. Tsurutani (Eds.)*
35 **Collisionless Shocks in the Heliosphere: Reviews of Current Research** *Bruce T. Tsurutani and Robert G. Stone (Eds.)*
36 **Mineral and Rock Deformation: Laboratory Studies—The Paterson Volume** *B. E. Hobbs and H. C. Heard (Eds.)*
37 **Earthquake Source Mechanics (Maurice Ewing Volume 6)** *Shamita Das, John Boatwright, and Christopher H. Scholz (Eds.)*

38 **Ion Acceleration in the Magnetosphere and Ionosphere** *Tom Chang (Ed.)*
39 **High Pressure Research in Mineral Physics (Mineral Physics Volume 2)** *Murli H. Manghnani and Yasuhiko Syono (Eds.)*
40 **Gondwana Six: Structure, Tectonics, and Geophysics** *Garry D. McKenzie (Ed.)*
41 **Gondwana Six: Stratigraphy, Sedimentology, and Paleontology** *Garry D. McKenzie (Ed.)*
42 **Flow and Transport Through Unsaturated Fractured Rock** *Daniel D. Evans and Thomas J. Nicholson (Eds.)*
43 **Seamounts, Islands, and Atolls** *Barbara H. Keating, Patricia Fryer, Rodey Batiza, and George W. Boehlert (Eds.)*
44 **Modeling Magnetospheric Plasma** *T. E. Moore and J. H. Waite, Jr. (Eds.)*
45 **Perovskite: A Structure of Great Interest to Geophysics and Materials Science** *Alexandra Navrotsky and Donald J. Weidner (Eds.)*
46 **Structure and Dynamics of Earth's Deep Interior (IUGG Volume 1)** *D. E. Smylie and Raymond Hide (Eds.)*
47 **Hydrological Regimes and Their Subsurface Thermal Effects (IUGG Volume 2)** *Alan E. Beck, Grant Garven, and Lajos Stegena (Eds.)*
48 **Origin and Evolution of Sedimentary Basins and Their Energy and Mineral Resources (IUGG Volume 3)** *Raymond A. Price (Ed.)*
49 **Slow Deformation and Transmission of Stress in the Earth (IUGG Volume 4)** *Steven C. Cohen and Petr Vaníček (Eds.)*
50 **Deep Structure and Past Kinematics of Accreted Terranes (IUGG Volume 5)** *John W. Hillhouse (Ed.)*
51 **Properties and Processes of Earth's Lower Crust (IUGG Volume 6)** *Robert F. Mereu, Stephan Mueller, and David M. Fountain (Eds.)*
52 **Understanding Climate Change (IUGG Volume 7)** *Andre L. Berger, Robert E. Dickinson, and J. Kidson (Eds.)*
53 **Plasma Waves and Istabilities at Comets and in Magnetospheres** *Bruce T. Tsurutani and Hiroshi Oya (Eds.)*
54 **Solar System Plasma Physics** *J. H. Waite, Jr., J. L. Burch, and R. L. Moore (Eds.)*
55 **Aspects of Climate Variability in the Pacific and Western Americas** *David H. Peterson (Ed.)*

Maurice Ewing Volumes

1 **Island Arcs, Deep Sea Trenches, and Back-Arc Basins** *Manik Talwani and Walter C. Pitman III (Eds.)*
2 **Deep Drilling Results in the Atlantic Ocean: Ocean Crust** *Manik Talwani, Christopher G. Harrison, and Dennis E. Hayes (Eds.)*
3 **Deep Drilling Results in the Atlantic Ocean: Continental Margins and Paleoenvironment** *Manik Talwani, William Hay, and William B. F. Ryan (Eds.)*
4 **Earthquake Prediction—An International Review** *David W. Simpson and Paul G. Richards (Eds.)*
5 **Climate Processes and Climate Sensitivity** *James E. Hansen and Taro Takahashi (Eds.)*
6 **Earthquake Source Mechanics** *Shamita Das, John Boatwright, and Christopher H. Scholz (Eds.)*

IUGG Volumes

1 **Structure and Dynamics of Earth's Deep Interior** *D. E. Smylie and Raymond Hide (Eds.)*
2 **Hydrological Regimes and Their Subsurface Thermal Effects** *Alan E. Beck, Grant Garven, and Lajos Stegena (Eds.)*
3 **Origin and Evolution of Sedimentary Basins and Their Energy and Mineral Resources** *Raymond A. Price (Ed.)*
4 **Slow Deformation and Transmission of Stress in the Earth** *Steven C. Cohen and Petr Vaníček (Eds.)*
5 **Deep Structure and Past Kinematics of Accreted Terranes** *John W. Hillhouse (Ed.)*
6 **Properties and Processes of Earth's Lower Crust** *Robert F. Mereu, Stephan Mueller, and David M. Fountain (Eds.)*
7 **Understanding Climate Change** *Andre L. Berger, Robert E. Dickinson, and J. Kidson (Eds.)*

Mineral Physics Volumes

1 **Point Defects in Minerals** *Robert N. Schock (Ed.)*
2 **High Pressure Research in Mineral Physics** *Murli H. Manghnani and Yasuhiko Syono (Eds.)*

PREFACE

This volume is an outgrowth of IUGG Union Symposium 9 held during the 1987 IUGG General Assembly at Vancouver, Canada. This symposium, jointly sponsored by IAVCEI, IASPEI, ICL and IAGA, consisted of 31 presentations ranging in subject matter from melt segregation and melt focusing processes beneath mid-ocean ridges, to the structures of oceanic crust and ophiolite analogues, morphological variations in the accretion process, the structural evolution of specific spreading ridge systems, the interplay between magmatism and rifting, and the chemical and thermal balances involved in mid-ocean ridge hydrothermal systems. Six of those papers have been expanded in the present volume.

These papers constitute several important advances in our understanding of the evolution of mid-ocean ridge systems. The recognition that transverse seismic anisotropy is an important characteristic of oceanic layer 2 (Fryer et al.) has profound implications for interpretations of crustal thicknesses based on seismic data, and appears to explain a long-standing enigma of marine seismology: the apparent thinning of upper crustal layers with age. An analysis of magnetic anomaly data and transform fault azimuths across the boundaries of the Pacific, Easter and Nazca plates (Naar and Hey) has resulted in the calculation of new, instantaneous plate motion models for a significant portion of the south Pacific plate boundaries, in addition to providing important constraints on the recent evolution of the Easter Microplate. A new kinematic model for the evolution of the Gorda Rise (Stoddard) reproduces the complex magnetic lineations of that area, and includes models for the generation of the President Jackson seamount chain. Phase equilibria are used to constrain the nature of magmas parental to differentiated lavas of Icelandic rift zones (Thy); these magmas contrast significantly with those for several other spreading ridges, with implications for the melting regimes operating there. The final two papers are devoted to evaluations of the accretion process over relatively short time intervals. The use of bottom observations at Axial Seamount on the Juan de Fuca Ridge has allowed Zonenshain et al. to decipher the volcanic, tectonic and hydrothermal history of this area over the last 60,000 years. An even finer scale view of the accretion process is provided by Jacoby et al., in their assessment of the implications of geophysical and geodetic data for magma movement in the Krafla Rift Zone, Iceland since 1975.

Collectively, these papers should lead to better understanding of the process of accretion at mid-oceanic ridges, and the structure and evolution of the oceanic crust produced in the plate boundary zone. The efforts of the following reviewers are gratefully acknowledged for their contributions to improving the manuscripts in this volume:

R. L. Chase	M. Fisk	K. C. Macdonald	D. Walker
N. Christiansen	R. N. Hey	B. Minster	G. P. L. Walker
P. Einarsson	J. Karsten	G. M. Purdy	D. S. Wilson

John M. Sinton
Honolulu, Hawaii

Evolution of Mid Ocean Ridges

CONTENTS

SEISMIC ANISOTROPY AND AGE-DEPENDENT STRUCTURE OF THE UPPER OCEANIC CRUST

Gerard J. Fryer, Daniel J. Miller[1], and Patricia A. Berge
Hawaii Institute of Geophysics, University of Hawaii at Manoa, Honolulu, Hawaii 96822

Abstract. Seismic anisotropy in oceanic layer 2 resulting from a preferred alignment of fractures has been widely recognized, but all experiments to date have sought to measure only the weak azimuthal variation of elastic properties resulting from tectonically controlled systems of vertical fractures. From ocean drilling data, however, especially from DSDP Hole 504B, we know that layer 2 is composed of interleaved massive flows and breccia units, and that the massive units have a very strong concentration of horizontal fractures. Layer 2's pronounced horizontal fabric of low-velocity "layers" (fractures and/or breccia zones) permeating an otherwise high-velocity matrix, will cause P-waves to travel faster horizontally than vertically. This anisotropy has no azimuthal expression, and so cannot easily be recognized in seismic data, but it may lead to overestimation of the thickness of upper crustal layers by as much as 30% in young crust. Further, the anisotropy affects P and S waves differently, so where shear-wave data are available, Poisson's ratio may be substantially underestimated. The widespread observation of a low Poisson's ratio zone in the upper few kilometers of young crust is almost certainly an artifact of ignoring anisotropy. As the crust ages, fractures and voids are filled by chemical alteration and precipitation, the velocity contrast between rock and void-filling material is reduced, and the anisotropy decreases. The errors introduced by assuming isotropy thus show an inverse relationship to crustal age, so that thickness measurements from old crust are probably no more than 10% in error. This explains a long-standing enigma of marine seismology: the apparent thinning of upper crustal layers with age.

Introduction

In a classic paper describing a compilation of a very large quantity of sonobuoy refraction data, Houtz and Ewing [1976] revealed two systematic age-dependent properties of the uppermost oceanic crust, layer 2A: its seismic velocities increase with age while its thickness decreases. Since that study, improved seismic data have demanded substantial modification of Houtz and Ewing's crude layer-cake interpretations [Spudich and Orcutt, 1980b], but the systematic increase of layer 2A velocities with age has been confirmed. In young crust layer 2A has low velocities but extremely strong velocity gradients [Bratt and Purdy, 1984; Purdy, 1987], while in older crust it has higher velocities and lower gradients [Purdy, 1983]. Lateral variability of structure may obscure this trend locally [Stephen, 1988], but the great body of marine seismic data, taken together, clearly shows that mean velocities follow Houtz and Ewing's trends.

The thinning of layer 2A is less well resolved. While Houtz and Ewing's statistics show clearly that 2A thins with age [Houtz and Ewing, 1976], subsequent seismic refraction surveys have not identified any age-dependent thickness on a regional scale. The failure of these more modern experiments, however, may result from investigation of too small an age range or proximity to confusing tectonics such as fracture zones. Only one series of refraction experiments has covered the range 0–10 M.y. in a region free of fracture zones, that of Bunch and Kennett [1980] on the Reykjanes Ridge. Bunch and Kennett saw not a thinning of layer 2A, but an equally puzzling thinning of the more constant velocity layer beneath, layer 2B.

The filling of fractures and pores in the shallow crust by alteration products and hydrothermal mineralization is generally believed to explain the increases in velocity with age and to be largely responsible for velocity gradients [Schreiber and Fox, 1976, 1977; Bratt and Purdy, 1984]. If such void filling makes the velocity age dependent, then it seems probable that it also controls the age dependence of the thickness of upper crustal layers. The obvious explanation for the thinning of layer 2A, that velocities increase through healing of voids until the layer cannot be resolved seismically from layer 2B, demands that layer 2B thicken while layer 2A thins. No such thickening is seen in seismic data. Indeed, on the Reykjanes Ridge, layer 2B is seen to thin by 500 m over 9 M.y. while the gradient zones of layers 2A and 2C remain fairly constant in thickness [Bunch and Kennett, 1980]. Clearly, a thinning layer underlain by a layer of constant thickness is incompatible with the idea of one layer growing at the expense of the other through hydrothermal deposition. It seems reasonable to assume that the rate at which crustal layers have been produced has not increased with time, but this leaves the observed thinning of upper crustal layers as an enigma.

Another enigma of marine seismology, apparently unrelated to the problem of thinning layers, is the seismic refraction observation of very low values of Poisson's ratio at depths of 1–3 km into the crust [Spudich and Orcutt, 1980a; Au and Clowes, 1984; Chiang and Detrick, 1985]. On the basis of laboratory measurements of ophiolite samples [Salisbury and Christensen, 1978; Christensen and Smewing, 1981], it is difficult to justify a Poisson's ratio of less than 0.26 anywhere in the crust, yet refraction data demand minima as low as 0.23. This disagreement is particularly troubling as it seems to represent a failure of the widely-held idea that ophiolites represent obducted sections of oceanic crust. Two explanations have been presented: (1) that the Poisson's ratio minima result from trondhjemites at much shallower levels and in much greater volume than they occur in ophiolites [Spudich and Orcutt, 1980a; Chiang and Detrick, 1985] (this

[1]now with the Department of Geological Sciences, AJ-20, University of Washington, Seattle, WA 98195

explanation itself violates the ophiolite analogue), and (2) that the minima are caused by much thicker cracks and much higher porosity than seems reasonable for these depths [Shearer, 1988]. Neither explanation is particularly convincing, and their authors seem quite willing to accept alternate explanations. The low values of Poisson's ratio have remained a puzzle.

We show here that the thinning of crustal layers, and the minima in Poisson's ratio, are apparent, not real. These anomalies are explained by the fabric of layer 2. Not only does the layering of extrusives impose a strong horizontal fabric on layer 2, but the geometry of fractures is critically important also. It is well accepted that the uppermost oceanic crust must be profoundly fractured, since only with large-scale porosity is it possible to reconcile P velocities of $5.9\,\mathrm{km\,s^{-1}}$ measured in drill samples of basement rocks [Hyndman and Drury, 1976] with seismic refraction observations of velocities as low as $2.1\,\mathrm{km\,s^{-1}}$ [Whitmarsh, 1978; Spudich and Orcutt, 1980a; Purdy, 1987]. Even with very high porosity it may be necessary to invoke pore pressure effects to explain such low seismic velocities [Spudich and Orcutt, 1980a; Christensen, 1984]. What has not been recognized is that fracture orientation too profoundly affects the seismic properties of the shallowest igneous crust.

That there are fractures with a preferred orientation in the oceanic crust is dramatically evident from any sidescan sonar image of a mid-ocean ridge [e.g., Fornari et al., 1988]. Such large-scale fractures are near vertical and introduce an azimuthal variation in seismic properties. Such fracture-induced azimuthal anisotropy was first detected by Stephen [1981], whose findings have since been extensively corroborated [White and Whitmarsh, 1984; Shearer and Orcutt, 1985; Stephen, 1985]. That another fracture set might coexist with the vertical fractures was completely unsuspected until Newmark et al. [1985] reported predominantly horizontal fractures occurring throughout layer 2 at DSDP site 504B (the fractures are indeed horizontal; Newmark et al. [1985] corrected for the fact that a vertical drill hole emphasizes horizontal features). Combined with the fabric imposed by flow layering, the horizontal fractures must induce a very strong seismic anisotropy such that compressional-wave energy travels faster in a horizontal direction than it does vertically. Standard refraction experiments cannot detect such anisotropy, however, so when upper crustal anisotropy is considered at all, it is invariably limited to the effects of vertical fractures. A natural consequence of this omission is that the thickness of crustal layers is systematically overestimated and Poisson's ratio underestimated. The anisotropy should decay with age, however, since it is primarily caused by voids and fractures which will fill as alteration and hydrothermal deposition continue. The errors in thickness should consequently also decay with age, making crustal layers appear to thin, while at the same time Poisson's ratio anomalies should appear to fall. Such behaviour is precisely what is observed.

Notation.

The notation of anisotropy is confusing so ambiguous terms abound in the literature. To keep things as intuitive as possible, we follow the recommendation of Crampin [1989] and use the term "azimuthal isotropy" to describe anisotropic systems which display no azimuthal variation of properties (the widely-used term "transverse isotropy," meaning isotropic transverse to some symmetry axis, is synonymous only when the symmetry axis is vertical). We find it helpful to define another term, "vertical anisotropy," meaning an anisotropic system in which there is variation of properties in any vertical plane; a vertically anisotropic medium need not be azimuthally isotropic (for example, an orthorhombic system is both vertically and azimuthally anisotropic).

Fractures, Fabric, and Velocity Variation

Layer 2 has a strongly-developed horizontal fabric, since it is made up of horizontally-lying thin flows, pillow units, massive lavas, and breccia zones, with intercalated sediment. This fabric is further enhanced by fractures: Newmark et al. [1985] report from televiewer (acoustical) images of the walls of Hole 504B that the pillows and massive units are extensively fractured, with the great predominance of fractures subhorizontal. A fabric displaying any preferred direction will render a medium anisotropic. We show the simplest possible fabrics in Figure 1, which shows media made up of high velocity particles imbedded in a low-velocity matrix. In Figure 1a the medium is random, displaying no preferred direction. A compressional wave impinging on a random medium "sees" the same bulk properties regardless of its direction, so its velocity is independent of direction. In contrast, a horizontal fabric (Figure 1b), will cause velocity to vary with angle of incidence. A P-wave travelling horizontally through the material of Figure 1b preferentially propagates through the higher velocity material, but a vertically travelling wave cannot avoid the lower velocity material, and so must travel at a lower "average" velocity. If the only fabric is horizontal, then velocity varies only with angle of incidence, and the medium is azimuthally isotropic.

Representative velocity variations in a vertical plane for isotropic and anisotropic media are shown in Figure 2. The exact form of the velocity variation for the anisotropic medium will depend on its elastic parameters; in general, azimuthal isotropy demands five elastic parameters to describe the velocity variation while isotropy requires only two. Note from Figure 2 that while the P-velocity is faster horizontally than vertically, the SV-velocity is the same in these directions. Note also that shear-wave triplications may occur (i.e., in certain directions, three SV arrivals may be detected).

A horizontal fabric results in vertical anisotropy, but the cause of that fabric is immaterial to the seismic response. Aligned fractures or pores, preferred orientation of grains, or any type of small-scale layering, will all result in anisotropy; these different causes will be seismically indistinguishable as long as the scale of the fabric is small compared to a seismic wavelength [Backus, 1962]. In seismic measurements of upper oceanic crust, the wavelength of a compressional wave is invariably greater than 50 m. This greatly exceeds the typical thickness of individual pillow, breccia, flow, or massive units: at DSDP Hole 504B, each unit is typically less than 5 m thick [Cann, Langseth, Honnorez, von Herzen, White, et al., 1983; Anderson, Honnorez, Becker, et al., 1985]. Although units as much as 50 m thick are observed,

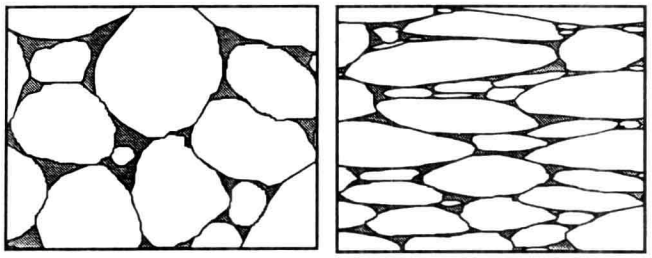

Fig. 1. A random medium (a) and the same medium foreshortened vertically so that it has a horizontal fabric (b). The particles have one velocity and the infilling matrix another. In (a), seismic velocities are independent of direction, but in (b), P waves will travel faster horizontally than vertically.

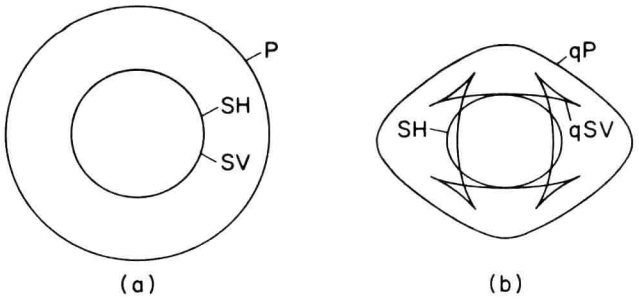

Fig. 2. Vertical sections of expanding wavefronts in (a) an isotropic medium and (b) a vertically anisotropic medium with azimuthal isotropy (the vertical axis is an axis of symmetry for both figures). In the isotropic medium both P and S wavespeeds are independent of direction, and the shear waves are degenerate, with SV and SH having the same speed. In the anisotropic medium, P and SH are faster horizontally than vertically while the speed of SV is the same in the horizontal and vertical directions. The SV wavefront may display triplications.

these are either subdivided into thinner subunits (such as individual pillows in a pillow lava sequence) or are moderately to severely disrupted by horizontal fractures [Newmark, et al., 1985], so that the entire thickness of layer 2 has a well-developed horizontal fabric with a characteristic scale length of a few meters. Other deep drill holes reveal similar fabric [e.g., Melson, Rabinowitz, et al., 1979; Donnelly, Francheteau, Bryan, Robinson, Flower, Salisbury, et al., 1980], but only 504B samples the deeper part of layer 2. It is clearly risky to extrapolate to the entire oceanic crust from a single drill hole, but since flows and pillows in ophiolites have similar dimensions to those inferred from site 504B [e.g., Casey, et al., 1981; Christensen and Smewing, 1981], we conclude that layer 2 does indeed have a well-developed horizontal fabric everywhere. Layer 2 must necessarily be vertically anisotropic.

Previous studies have not seriously considered the possibility of layer 2 anisotropy other than the azimuthal variability imposed by vertical fractures. Whitmarsh [1978] casually noted that anisotropy might result from the multiple layering of flows, and Newmark et al. [1985] observed that the horizontal fractures seen in televiewer data should make the medium strongly anisotropic, but the matter has not been pursued because no vertical anisotropy has been observed in seismic data.

That vertical anisotropy has not been identified in layer 2 demands some explanation. Vertical anisotropy has been widely identified in marine sediments [Bachman, 1979], principally from laboratory measurements. The in situ identification of such anisotropy has only been possible in sedimentary formations where the same identifiable horizon exists in both reflection and refraction data [e.g., Davis and Clowes, 1986], or when depths computed from reflection data disagree with depths obtained directly by drilling [e.g., Banik, 1984]. In the case of layer 2, the sample size for laboratory measurement of velocity from core samples is too small to sample the seismic effects of fractures or fabric, while the lack of a uniform prominent reflecting/refracting horizon in the upper crust means that a mismatch between reflection and refraction results, indicative of vertical anisotropy, has never been noticed. By contrast, anisotropy induced by vertical fractures which has been widely observed in layer 2 [Stephen, 1981, 1985; White and Whitmarsh, 1984; Shearer and Orcutt, 1985]. Vertical fracturing gives rise to an azimuthal anisotropy which can be detected seismically by shooting a circle around a receiver and mapping the variation of properties with direction. Vertical anisotropy arising from a horizontal fabric displays no such azimuthal variation.

Although it has not been observed, the vertical anisotropy is probably very large. The very high fracture concentrations reported by Newmark et al. [1985], together with the high contrast in seismic velocity between unfractured basalt and fracture-filling water, imply a very strong anisotropy dominated by fracture-induced effects. Extrapolating from the results of Anderson et al. [1974] it seems likely that in areas where there is little hydrothermal deposition the fracture-induced anisotropy approaches 40% for P-waves.

Velocity Gradients and Vertical Anisotropy

Where vertical anisotropy occurs in a region of velocity increase with depth, the effects of the two phenomena, anisotropy and velocity gradient, are intrinsically coupled; one cannot be considered at the exclusion of the other. In the oceanic crust, velocity gradients are greatest in the upper two kilometers, in the same depth range where fractures and fabric suggest appreciable anisotropy. Unfortunately, marine seismic experiments sample this part of the crust inadequately. Our knowledge of seismic structure is gleaned almost entirely from sparse, poor quality P-refraction data. These data can always be explained adequately without invoking anisotropy, but the final models resulting from such analysis, while self-consistent, may be profoundly wrong, as we shall show.

We illustrate the problem schematically in Figure 3. A horizontally-fractured ocean crust, in which velocities and aligned fracture concentration both increase with depth, has a velocity-depth dependence something like the heavy curves in Figure 3c. At any given depth, the velocity of horizontally travelling P waves, v_{PH}, is higher than that of vertically travelling waves, v_{PV}. Regardless of the degree of

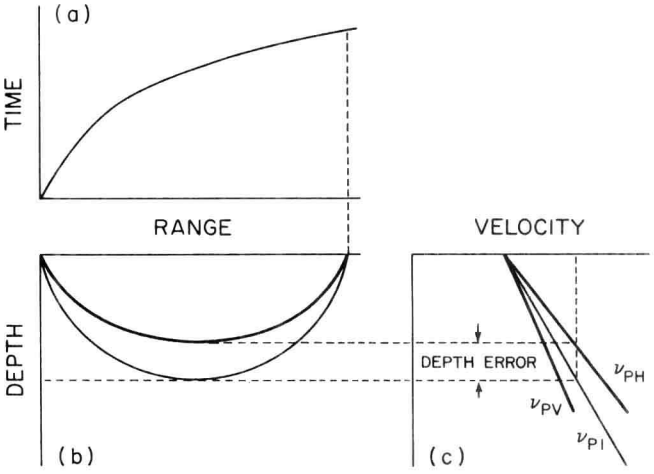

Fig. 3. Errors in depth determinations.
(a) P-refraction travel time plot for source and receiver on a horizontally fractured ocean bottom with a velocity gradient.
(b) The true raypath through the anisotropic medium (heavy curve) and the raypath assumed by any isotropic inversion procedure (light curve).
(c) The true velocity-depth function (heavy lines); v_{PH} is horizontal velocity, v_{PV} is vertical velocity. The inversion procedure picks the light line labelled v_{PI}.

fracture-induced anisotropy, from P-refraction data alone it will be impossible to detect any anisotropy at all. The travel-time curve for P-refractions, Figure 3a, gives no indication of anisotropy, but in an actual experiment, this travel-time curve will comprise the only information available. Invariably, isotropy will be assumed. Inversion to obtain a velocity-depth function proceeds by determining the horizontal velocity at a turning point (from the slope of the travel-time curve of Figure 3a), then adjusting depths to satisfy travel times. With no indication of anisotropy, we can only assume that velocities are the same in all directions. If, as in this case, vertical P velocities are really less than horizontal, then a ray will not penetrate to as great a depth to yield the same travel time. A refracted ray will have a shallower turning point than the ray implicitly assumed by the inversion scheme, as shown in Figure 3b. Figure 3c shows the consequences of this depth difference for the inversion. The velocity-depth function deduced from travel-time analysis, v_{PI}, lies somewhere between the true vertical and horizontal velocities. Since the v_{PI} curve always lies below the v_{PH} curve, seismic refraction data will systematically overestimate depths.

Age Dependence

We have suggested above that the apparent thinning of crustal layers with age results from a reduction in anisotropy. To investigate this we have considered a series of upper crustal models loosely based on the idealized structure of Bratt and Purdy [1984], modified to include the anisotropic effects of horizontal fractures and varying degrees of fracture filling. The objective here was to see how realistic degrees of anisotropy may have contributed to misinterpretation of seismic data.

The first model, representing young crust ("Age Zero"), is shown by the first of the diagrams in Figure 4. This model has 8% anisotropy at the top of layer 2A, increasing to 35% at the base of layer 2A, at a depth of 500 m below the seafloor. Such increase in anisotropy with depth is broadly consistent with the observation that fracture density increases with depth in layer 2A [Newmark et al., 1985], but such large anisotropy would only be possible if the cracks were predominantly water-filled. In layer 2B of the model (500–1000 m depth), velocities and anisotropy increase more slowly with depth. In layer 2C (1000–1500 m depth) the anisotropy decreases, consistent with the idea that fractured flows progressively give way to unfractured dikes as depth increases. Throughout the entire model, elastic parameters were chosen to be consistent with a horizontally-fractured medium, following the theory of Schoenberg [1983].

We computed P travel times for this vertically anisotropic structure and then inverted them, assuming isotropy, using the τ-sum method of Diebold and Stoffa [1981]. The line labelled v_{PI} in Figure 4 shows the inversion results. Because of the depth errors intrinsic to the assumption of isotropy, layer 2A thickness has been overestimated by over 100 m and overall layer 2 thickness by almost 400 m. Ignoring the anisotropy has introduced errors of about 25%.

As the crust ages, alteration products and hydrothermal deposits fill the cracks, with mineralization growing inward from the walls of the crack. This reduces crack dimensions and so increases the overall seismic velocity. The mineralization also changes the crack aspect ratios: as the deposits on the walls grow, cracks and fractures will get proportionately thinner (the aspect ratios will decrease), until bridging between the walls occurs to produce isolated void spaces each with larger aspect ratio (i.e., closer to spherical) than the original fracture. With both crack thinning and bridging going on, it is not at all clear how the mean aspect ratio will vary. Although anisotropy is sensitive to aspect ratio [Shearer, 1988], we expect that any anisotropy change related to a change in mean aspect ratio will be much smaller than the decrease in anisotropy resulting from the reduction in velocity contrast between rock and crack-filling material. Overall, velocities will increase while gradients and anisotropy decrease.

To investigate the consequences of these time dependent effects, we have assumed a linear change in the elastic stiffnesses with "time," and performed the same ray-tracing and inversion exercise described above for "Age Zero" for a variety of older models, also shown in Figure 4: "Age Five" has a maximum anisotropy of 20%, and "Age Ten" a maximum anisotropy of 8%. As expected, as the anisotropy decreases, the depth errors introduced by assuming isotropic structure also decrease.

Since the depth errors decrease as a function of the amount of fracture filling, crustal layers will appear to thin with age. Figure 5 demonstrates this result for all of layer 2. The apparent thinning is completely consistent with Bunch and Kennett's [1980] measurements on the Reykjanes Ridge. Figure 6 shows the apparent thinning just for layer 2A; the curve is remarkably similar to Houtz and Ewing's [1976] results. While Houtz and Ewing [1976] suggested that layer 2A thins to zero thickness, the resolution of their data was probably only about 500 m, so the apparent thinning we predict quite adequately explains their observations.

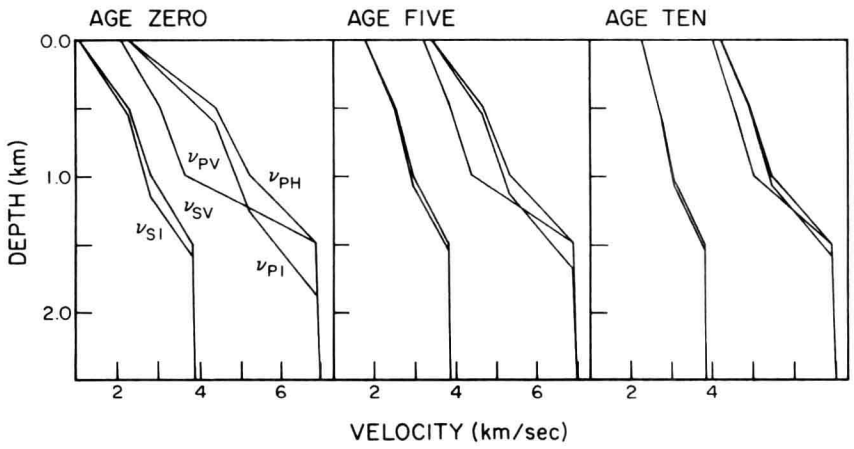

Fig. 4. Velocity-depth functions for young (Age Zero), intermediate (Age Five) and old (Age Ten) oceanic crust. Layers 2A, 2B and 2C comprise the depth range 0–500 m, 500–1000 m and 1000–1500 m respectively. Two curves define the P velocity in each case: v_{PV} for vertical propagation and v_{PH} for horizontal propagation. True shear velocity, v_{SV}, is marked by a single curve, as both vertically and horizontally travelling SV waves have the same speed. Gradients are high and anisotropy (apparent from the separation of the v_P curves) is initially low in Layer 2A. Fracture concentration increases through 2A so anisotropy increases. Layer 2B has a much lower gradient and near-uniform anisotropy. Fracture concentration (and hence anisotropy) falls through Layer 2C and is zero in Layer 3. Curves v_{PI} and v_{SI} show the inversions which would be obtained if the structures were assumed to be isotropic and P and S travel times were inverted separately. Note that the P and S inversions disagree in depth. The errors in the P-inversions decrease with age as the anisotropy decreases due to fracture filling.

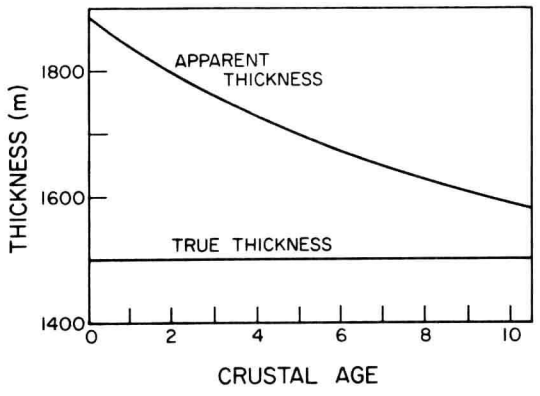

Fig. 5. Apparent thinning of Layer 2 with "age." The true thickness is constant but the layer appears to thin because the errors introduced by anisotropy decrease as the anisotropy decreases.

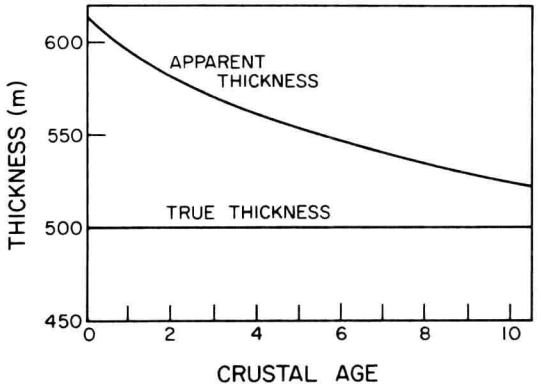

Fig. 6. Apparent thinning of Layer 2A with "age." If the resolution of seismic data were poorer than 500 m, the layer would appear to thin to zero thickness, as suggested by Houtz and Ewing [1976].

Shear Waves and Poisson's Ratio

Shear-wave velocity variations in an azimuthally isotropic medium are quite different from the compressional variation, as we have seen in Figure 2. An important point to note from Figure 2 is that vertically and horizontally propagating SV waves have the same velocity (even though the velocity may be different in some other direction). Consequently, inversions of shear-wave refraction data produce much smaller depth errors than those suffered in a P inversion. This can be seen in Figure 4 by comparing the v_{PI} and v_{SI} curves with the true structure.

Since the P and S depth errors differ, if isotropic inversions are believed, an S velocity from one depth will be associated with a P velocity which actually belongs to some shallower depth; the P velocity will seem to be too small. Any quantity depending on both P and S velocities will display anomalous behaviour. One such quantity is Poisson's ratio σ, which, for an isotropic material, is given by

$$\sigma = \frac{1}{2}\left[\frac{v_P^2 - 2v_S^2}{v_P^2 - v_S^2}\right],$$

where v_P and v_S are P and S velocities. Since the P velocity is too small for the S velocity, Poisson's ratio will be systematically underestimated. This is illustrated in Figure 7, which shows both the true Poisson's ratio and the apparent Poisson's ratios deduced from the isotropic inversions of Figure 4.

It is apparent that if the upper crust has vertical anisotropy, we should expect to find anomalously low Poisson's ratios when we interpret seismic refraction data assuming isotropy. Such anomalies are widely observed. Figure 8 shows the apparent Poisson's ratio trajectory of Spudich and Orcutt [1980a] for 15 M.y.-old crust. The curve shows a distinct minimum of $\sigma = 0.24$ at a depth of about 1.4 km. Au and Clowes [1984] and Chiang and Detrick [1985] have found similar Poisson's ratio minima. In all of these cases, the true cause of the Poisson's ratio minimum is probably a misinterpretation of the seismic data. The assumption of isotropy forces us to compare P and S velocities from different depths and a low Poisson's ratio is a necessary consequence. We have made no attempt to model the Spudich and Orcutt [1980a] result shown in Figure 8, yet its similarity to the Age Five curve of Figure 7 is so remarkable that we are confident enough to assert that the crust at Spudich and Orcutt's site contains partially-filled horizontal fractures down to 1.5 km depth.

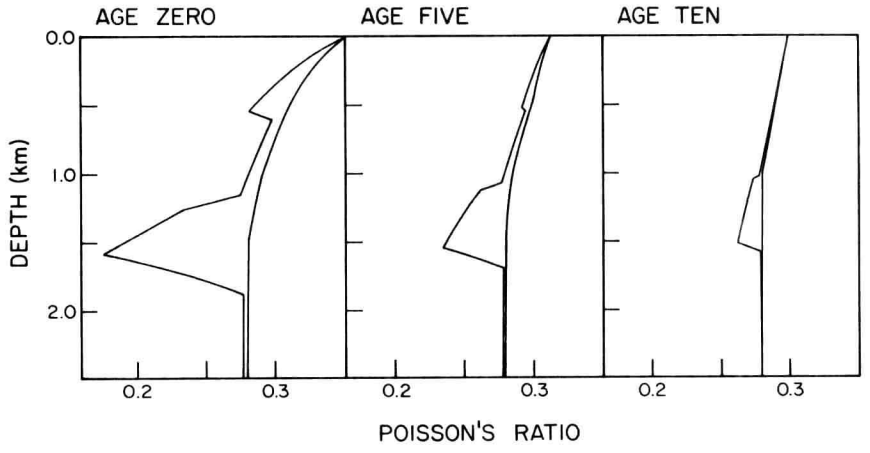

Fig. 7. Poisson's ratio as a function of depth for the structures of Figure 4. The heavy curves show the correct (horizontal) Poisson's ratios, the light curves show the Poisson's ratios that would be inferred from the isotropic inversions. Note that the apparent Poisson's ratio is systematically too low, but that the error decreases with age.

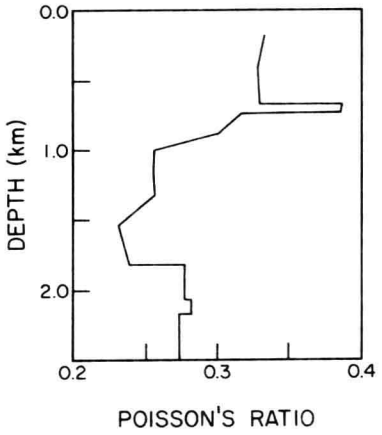

Fig. 8. Apparent Poisson's ratio curve from Spudich and Orcutt [1980a]. Poisson's ratio appears to reach a minimum of about 0.24 at about 1.5 km depth. Compare this minimum with that for the Age Five structure in Figure 7.

As final evidence that vertical anisotropy explains the Poisson's ratio minima we consider Shearer and Orcutt's [1986] refraction results from 140 M.y.-old lithosphere in the Western Pacific. These authors measured azimuthal anisotropy in the upper crust, almost certainly the result of vertical fractures, but they did not consider the possibility of any superimposed vertical anisotropy caused by horizontal fractures. Nevertheless, convincing evidence for such anisotropy exists within their published results. After a very careful travel-time analysis, Shearer and Orcutt were unable to reconcile the P and S-wave data: their S-wave profile reaches layer 3 velocities at 1.7 km depth versus 2 km for the P-velocity profile. This is a classic case of overestimation of depth from P-wave data indicative of vertical anisotropy. If we combine Shearer and Orcutt's P and S profiles we obtain a Poisson's ratio minimum of about 0.26 at a depth of 1.7 km, very similar to but slightly deeper than the anomaly for the Age Ten crust in Figure 4. We conclude that the crust at Shearer and Orcutt's site is horizontally fractured, but that the fractures are substantially more filled than at Spudich and Orcutt's [1980a] 15 M.y.-old site. It is worth noting that if we demand that the layer 2-layer 3 boundary be at the same depth for both P and S waves, then Shearer and Orcutt's data are incompatible with a vertically isotropic upper crust.

Discussion

We have argued that alteration and hydrothermal deposition will change the geometry of fractures and other voids through time and so modify the seismic structure of the upper crust. While age will be the controlling factor in determining the degree of healing of cracks through low-temperature alteration [Schreiber and Fox, 1977], the effects of hydrothermal deposition will depend more on the distribution and vigor of hydrothermal circulation cells than on age per se. We should expect that in areas of vigorous hydrothermal activity the modification of crack volume and aspect ratio by mineralization will result in low anisotropy and increased seismic velocities, regardless of age. Since hydrothermal circulation must vary both along and across strike, we should expect lateral heterogeneity in the upper crust. Such heterogeneity is indeed observed [Stephen, 1988]. The arbitrary "age" of Figures 4–7 is thus in part really some cumulative measure of hydrothermal deposition.

The fact that there is both apparent thinning and a reduction in the Poisson's ratio anomaly with age confirms what we have already suggested, that the vertical anisotropy arises primarily from the horizontal fractures rather than from the fabric of superposed flows. Anisotropy resulting purely from the fabric of the layering must be independent of age, while fracture-induced anisotropy will show an age dependence because of the time-dependent void geometry. Even completely filled fractures would produce some residual anisotropy, because of the velocity contrast between fracture-filling material and the unfractured basalt. The oceanic crust probably never attains complete fracture filling, however: even in old crust, porosity is high [Purdy, 1987], so it is probable that fractures too are only partially filled. Very crude estimates based on the anisotropy implied by Shearer and Orcutt's [1986] structure (the one datum we have from old crust) suggest that the fractures are only half-filled by 140 M.y. age. Since the partial filling of fractures yields such a clear age dependence, we suspect that fractures produce almost all of the anisotropy, and that the effects of non-fracture fabric are negligible.

We have not yet discussed the origins of the fracturing. Newmark et al. [1985] suggest two possible causes for fractures at Hole 504B: natural hydrofracturing of wet rock during dike injection, and mechanical rebound with brittle failure immediately following the intrusion of a dike into rock under high tension. We regard natural hydrofracturing as the more plausible mechanism. The argument here is that thermal pressurization of water during dike injection can be adequate to cause the host rock to fail, especially the more massive and less porous units. Newmark et al. [1985] applied Hole 504B physical properties to the theory of Delaney [1982] and determined that horizontal stresses would be greater than vertical stresses, explaining the very shallow dip of the fractures. If that is indeed the mechanism, then the same phenomenon probably occurs at all spreading centers, making horizontal fractures a ubiquitous feature of shallow ocean crust.

While we believe that we have presented here a strong case for vertical anisotropy in the shallow crust, it is important to note that we have not yet performed an actual inversion of seismic data to show that such anisotropy must exist. We have simply hypothesized particular styles of anisotropy consistent with televiewer observations and showed that vertical anisotropy provides more plausible explanations for seismic refraction data than more traditional isotropic models. The best technique to measure this anisotropy would be to use downhole seismometers and vertical seismic profiling, but this clearly could only be done at a drill hole and then would only provide measurements at a single point. For studies of age dependence or along-axis variation multiple drill holes would be required, a prohibitive expense. Unfortunately, the direct measurement of vertical anisotropy from traditional ocean-bottom seismometer refraction data is not possible, as the inverse problem is underconstrained if only P and SV refractions are recorded. With additional information, however, either P and SV reflections from some horizon beneath the anisotropic layers, or SH refractions, or preferably both, stable inversion is possible [Miller et al., 1987]. Shear wave information is critical, and for this reason the use of ocean-bottom seismometers in marine refraction experiments should be encouraged. The value of SH information means that serious consideration should be given to the development of on-bottom shear wave sources capable of putting enough energy into the bottom to sample depths of up to two kilometers.

A single experiment would provide a measure of the anisotropy at a point, but determining the age dependence requires a series of experiments. Because of the along-axis variability of spreading style, measurements must be made along a single seafloor spreading flow line. The global age relationships described by Houtz and Ewing [1976], layer thinning and velocity increases, were not apparent in measurements made on 0.5 and 4.0 M.y.-old crust in the ROSE area [Purdy, 1982], but those measurements were taken on crust formed at

different segments of a rise axis. By contrast, using measurements at 0, 3 and 9 M.y. age along a single flow line on the Reykjanes Ridge, Bunch and Kennett [1980] were able to confirm the Houtz and Ewing trends. Following the same sampling philosophy, to investigate the age dependence of the anisotropy, we recommend small-scale on-bottom experiments at three or more locations on 0-to-10 M.y.-old crust along a single flow line.

We have discussed here only vertical anisotropy resulting from horizontal layering and fractures. Since the vertical fractures in the crust also induce an anisotropy, the actual anisotropy of the crust must have contribution from both systems. The velocity variation resulting from vertical fractures alone has a hexagonal symmetry with a horizontal symmetry axis aligned perpendicular to the fractures [Crampin, 1978; Schoenberg, 1983]. In seismic experiments the symmetry axis is typically found to be parallel to the spreading direction [e.g., Stephen, 1985], implying that the vertical fractures are perpendicular to spreading, as expected from tectonics. With such symmetry there will be no anisotropy perpendicular to spreading, but there will be anisotropy in all other vertical planes. Most of the refraction lines we have considered here were perpendicular to spreading, so vertical fractures cannot explain the vertical anisotropy we have detected. The fact that vertical fractures will give rise to a vertical anisotropy along other azimuths, however, emphasizes the need to know the alignment of refraction lines relative to local tectonic features. It is clear that any quantitative investigation of anisotropy in the oceanic crust must admit the possibility of both vertical and horizontal fracture systems and so should measure the full three-dimensional variation of velocity with direction.

Conclusions

Horizontal fractures within layer 2 render the layer anisotropic, but the anisotropy has no azimuthal expression and so cannot easily be detected seismically. A simple assessment of the effects of this anisotropy shows that two major enigmas of marine seismology, the thinning of upper crustal layers with age and the existence of a zone of anomalously low Poisson's ratio, are really artifacts resulting from the erroneous assumption that the crust is isotropic. Expanding seismic wavefronts are distorted by the anisotropy; in particular, P wavefronts are distorted such that layers appear to be thicker than they really are. The apparent thinning of layers indicates a decay of anisotropy with age (and hence a reduction in wavefront distortion) resulting from the filling of the fractures by alteration products and hydrothermal precipitation. This suggests that studies of the anisotropy should yield information on the nature and longevity of hydrothermal systems.

The wavefront distortion resulting from the fractures is different for P and S waves, so the combination of P and S data to get Poisson's ratio yields erroneous values which are systematically too small. Low Poisson's ratios are never seen in ophiolites, so the demonstration that the Poisson's ratio anomalies are artifacts is particularly important: the major inconsistency between the ophiolite model of the ocean crust and seismic refraction data has been removed.

The only direct evidence we have for the horizontal fracturing is from the borehole televiewer imagery of Newmark et al. [1985]. There have been other televiewer lowerings in ocean drill holes, but all other published images have been degraded by ship motion. New digitally recording televiewers are now available which permit post-log image reconstruction. Use of these new instruments, and display of the resulting data as travel-time images as well as the traditional amplitude images, should greatly enhance the identification of fractures. The use of such devices (with heave compensation if seas are too large) should be encouraged in every drill hole penetrating more than 50 m into igneous crust.

We do not yet know how to measure the fracture-induced anisotropy directly, although it is clear that a successful experiment will have to use on-bottom sources and ocean bottom (or downhole) seismometers. In the meantime, it is essential that the possibility of anisotropy be kept in mind during analysis of seismic refraction data from the oceans. While the anisotropy resulting from vertical fractures can be avoided by orienting refraction lines perpendicular to the spreading direction, it is impossible to escape the anisotropic effects of horizontal fractures. Even when this vertical anisotropy is small, the assumption of isotropy can lead to significant errors in depth. To avoid such errors, inversion of seismic data should be guided by comparing field seismograms to synthetics which include the effects of azimuthal isotropy (computed, for example, following the techniques of Fryer and Frazer [1987]). If such synthetic seismogram software is unavailable, analysing P and S data separately will at least preserve the differences in structure from which a departure from isotropy can be estimated. The most convincing of the evidence presented here for this anisotropy are the depth disagreements between P and S data made evident in the Poisson's ratio minima of Spudich and Orcutt [1980a], Au and Clowes [1984], and Shearer and Orcutt [1986]. Driven by a desire to match their data as accurately as possible, these authors resisted the temptation to force similar features in their P and S profiles to occur at the same depths; from the curious structures resulting from their analyses, vertical anisotropy can confidently be inferred. It is likely, however, that the interpretation of data from other refraction experiments, especially in older crust, has implicitly assumed isotropy by forcing all interfaces in the structure to be at the same depth in both P and S profiles. It seems probable that there is much to learn about anisotropy, (and, by inference, about hydrothermal systems and crustal ageing), from seismic data already in existence.

Acknowledgments. This research was supported by the Office of Naval Research and from National Science Foundation grants OCE-8516225 and OCE-8711646. Hawaii Institute of Geophysics contribution no. 2095.

References

Anderson, D. L., B. Minster, and D. Cole, The effects of oriented cracks on seismic velocities, *J. Geophys. Res., 79,* 4011–4015, 1974.

Anderson, R. N., J. Honnorez, K. Becker, et al., Hole 504B, Leg 83, *Initial Rep. Deep Sea Drill. Proj., 83,* 13–118, 1985.

Anderson, R. N., H. O'Malley, and R. L. Newmark, Use of geophysical logs for quantitative determination of fracturing, alteration, and lithostratigraphy in the upper oceanic crust, Deep Sea Drilling Project, Holes 504B and 556, *Initial Rep. Deep Sea Drill. Proj., 83,* 443–478, 1985.

Au, D., and R. M. Clowes, Shear-wave velocity structure of the oceanic lithosphere from ocean bottom seismometer studies, *Geophys. J. R. Astron. Soc., 77,* 105–123, 1984.

Bachman, R. T., Acoustic anisotropy in marine sediments and sedimentary rocks, *J. Geophys. Res., 84,* 7661–7663, 1979.

Backus, G. E., Long-wave elastic anisotropy produced by horizontal layering, *J. Geophys. Res., 67,* 4427–4440, 1962.

Banik, N. C., Velocity anisotropy of shales and depth estimation in the North Sea basin, *Geophysics, 49,* 1411–1419, 1984.

Bratt, S. R., and G. M. Purdy, Structure and variability of oceanic crust on the flanks of the East Pacific Rise between 11° and 13°N, *J. Geophys. Res., 89,* 6111–6125, 1984.

Bunch, A. W. H., and B. L. N. Kennett, The crustal structure of the Reykjanes Ridge at 59°30′N, *Geophys. J. R. Astron. Soc., 61,* 141–166, 1980.

Cann, J. R., M. G. Langseth, J. Honnorez, R. P. Von Herzen, S. M.

White, et al., Sites 501 and 504: sediments and ocean crust in an area of high heat flow on the southern flank of the Costa Rica Rift, *Initial Rep. Deep Sea Drill. Proj., 69,* 31–173, 1983.

Casey, J. F., J. F. Dewey, P. J. Fox, J. A. Karson, and E. Rosencrantz, Heterogeneous nature of oceanic crust and upper mantle: a perspective from the Bay of Islands ophiolite complex, in *The Sea,* vol. 7, *The Oceanic Lithosphere,* edited by C. Emiliani, pp. 305–338, J. Wiley & Sons, New York, 1981.

Christensen, N. I., Pore pressure and oceanic crustal seismic structure, *Geophys. J. R. Astron. Soc., 79,* 411–423, 1984.

Christensen, N. I., and J. D. Smewing, Geology and seismic structure of the northern section of the Oman ophiolite, *J. Geophys. Res., 86,* 2545–2555, 1981.

Chiang, C. S., and R. S. Detrick, The structure of the lower oceanic crust from synthetic seismogram modeling of near-vertical and wide-angle reflections and refractions near DSDP site 417 in the Western North Atlantic (abstract), *Eos, Trans. Am. Geophys. Union, 66,* 956, 1985.

Crampin, S., Seismic wave propagation through a cracked solid: polarization as a possible dilatancy diagnostic, *Geophys. J. R. Astron. Soc., 53,* 467–496, 1978.

Crampin, S., Suggestions for a consistent notation for seismic anisotropy, *Geophys. Prospecting,* in press, 1989.

Davis, E. E., and R. M. Clowes, High velocities and seismic anisotropy in Pleistocene turbidites off Western Canada, *Geophys. J. R. Astron. Soc., 84,* 381–399, 1986.

Delaney, P. T., Rapid intrusion of magma into wet rock: groundwater flow due to pore pressure increases, *J. Geophys. Res., 87,* 7739–7756, 1982.

Diebold, J. B., and P. L. Stoffa, The traveltime equation, tau-*p* mapping, and inversion of common midpoint data, *Geophysics, 46,* 238–254, 1981.

Donnelly, T., J. Francheteau, W. Bryan, P. Robinson, M. Flower, M. Salisbury, et al., Site 418, *Initial Rep. Deep Sea Drill. Proj., 51–53, Part 1,* 351–626, 1980.

Fryer, G. J., and L. N. Frazer, Seismic waves in stratified anisotropic media – II. Elastodynamic eigensolutions for some anisotropic systems, *Geophys. J. R. Astron. Soc., 91,* 73–101, 1987.

Fornari, D. J., J. A. Madsen, D. G. Gallo, M. R. Perfit, and A. N. Shor, Morphology of the East Pacific Rise from the axis to seafloor ~4 ma old between 13°–15° N: Bathymetric anomalies and local variations in subsidence along a ridge segment (abstract), *Eos, Trans. Am. Geophys. Union, 69,* 1485, 1988.

Houtz, R., and J. Ewing, Upper crustal structure as a function of plate age, *J. Geophys. Res., 81,* 2490–2498, 1976.

Hyndman, R. D., and M. J. Drury, The physical properties of oceanic basement rocks from deep drilling on the Mid-Atlantic Ridge, *J. Geophys. Res., 81,* 4042–4052, 1976.

Melson, W. G., P. D. Rabinowitz, et al., Site 395: 23°N Mid-Atlantic Ridge, *Initial Rep. Deep Sea Drill. Proj., 45,* 131–264, 1979.

Miller, D. J., G. J. Fryer, and P. A. Berge, Measurement of transverse isotropy in marine sediments: what data are required? (abstract), *Eos, Trans. Am. Geophys. Union, 68,* 1375, 1987.

Newmark, R. L., R. N. Anderson, D. Moos, and M. D. Zoback, Sonic and ultrasonic logging of Hole 504B and its implications for the structure, porosity, and stress regimes of the upper 1 km of the oceanic crust, *Initial Rep. Deep Sea Drill. Project, 83,* 479–510, 1985.

Purdy, G. M., The variability in seismic structure of layer 2 near the East Pacific Rise at 12°N, *J. Geophys. Res., 87,* 8403–8416, 1982.

Purdy, G. M., The seismic structure of 140 Myr old crust in the western central Atlantic Ocean, *Geophys. J. R. Astron. Soc., 72,* 115–137, 1983.

Purdy, G. M., New observations of the shallow seismic structure of young oceanic crust, *J. Geophys. Res., 92,* 9351–9362, 1987.

Salisbury, M. H., and N. I. Christensen, The seismic velocity structure of a traverse through the Bay of Islands ophiolite complex, Newfoundland, an exposure of oceanic crust and upper mantle, *J. Geophys. Res., 83,* 805–817, 1978.

Schreiber, E., and P. J. Fox, Compressional wave velocities and mineralogy of fresh basalts from the Famous area and the Oceanographer Fracture Zone and the texture of layer 2A of the oceanic crust, *J. Geophys. Res., 81,* 4071–4076, 1976.

Schreiber, E., and P. J. Fox, Density and *P*-wave velocity of rocks from the FAMOUS region and their implication to the structure of the oceanic crust, *Geol. Soc. Am. Bull., 88,* 600–608, 1977.

Schoenberg, M., Reflection of elastic waves from periodically stratified media with interfacial slip, *Geophys. Prospecting, 31,* 265–292, 1983.

Shearer, P. M., Cracked media, Poisson's ratio and the structure of the upper oceanic crust, *Geophys. J., 92,* 357–362, 1988.

Shearer, P. M., and J. A. Orcutt, Anisotropy in the oceanic lithosphere – theory and observations from the Ngendei seismic refraction experiment in the south-west Pacific, *Geophys. J. R. Astron. Soc., 80,* 493–526, 1985.

Shearer, P. M., and J. A. Orcutt, Compressional and shear wave anisotropy in the oceanic lithosphere — the Ngendei seismic refraction experiment, *Geophys. J. R. Astron. Soc., 87,* 967–1003, 1986.

Spudich, P., and J. Orcutt, Petrology and porosity of an oceanic crustal site: Results from waveform modeling of seismic refraction data, *J. Geophys. Res., 85,* 1409–1433, 1980a.

Spudich, P., and J. Orcutt, A new look at the seismic velocity structure of the oceanic crust, *Rev. Geophys. and Space Phys., 18,* 627–645, 1980b.

Stephen, R. A., Seismic anisotropy observed in upper oceanic crust, *Geophys. Res. Letters, 8,* 865–868, 1981.

Stephen, R. A., Seismic anisotropy in the upper oceanic crust, *J. Geophys. Res., 90,* 11383–11396, 1985.

Stephen, R. A., Lateral heterogeneity in the upper oceanic crust at DSDP Site 504, *J. Geophys. Res., 93,* 6571–6584, 1988.

White, R. S., and R. B. Whitmarsh, An investigation of seismic anisotropy due to cracks in the upper oceanic crust at 45°N, Mid-Atlantic Ridge, *Geophys. J. R. Astron. Soc., 79,* 439–467, 1984.

Whitmarsh, R. B., Seismic refraction studies of the upper igneous crust in the North Atlantic and porosity estimates for layer 2, *Earth and Planet. Sci. Letters, 37,* 451–464, 1978.

RECENT PACIFIC-EASTER-NAZCA PLATE MOTIONS

David F. Naar[1] and R. N. Hey

Hawaii Institute of Geophysics
School of Ocean and Earth Science and Technology
University of Hawaii, Honolulu, Hawaii 96822

Abstract. Instantaneous relative plate motions have been calculated for the Pacific, Easter and Nazca plates by inverting spreading rates since the Brunhes/Matuyama reversal boundary (obtained from modeling 39 magnetic anomaly profiles across the divergent boundaries of all three plates), along with 10 transform azimuths (obtained from recent SeaMARC II, GLORIA and Sea Beam data) and 20 published seismic slip vectors. The rates along the Nazca–Pacific and Nazca–Easter spreading axes increase to the south. The rates along the Pacific–Easter spreading axis decrease to the south. Along ~2400 km of the southern Nazca–Pacific plate boundary where spreading rates range from 145 to 160 km there are no Nazca–Pacific transform faults where spreading axes are offset. Instead, the offsets are accommodated by microplates, propagating rifts, or overlapping spreading centers. The origin of the Easter microplate cannot be attributed solely to fast spreading rates along the preexisting Nazca–Pacific boundary because the fastest seafloor spreading is to the south of the microplate. The Nazca–Pacific Euler vector (0–0.73 Ma) from this study has a slower angular velocity and lies outside the confidence ellipse of the Minster and Jordan RM2 Euler vector (0–3.0 Ma). It also lies outside of the confidence ellipse of the DeMets et al. NUVEL-1 Euler vector (0–3.0 Ma) but has approximately the same angular velocity. Our preferred Euler vector describing the absolute motion of the Easter microplate is near the center of the microplate with an angular velocity of about 15°/m.y., making it a fast 'spinning' plate. Oblique convergence is predicted along the proposed Nazca–Easter and Pacific–Easter transform segments of the proposed northern and southern triple junctions, respectively. The similarity between the best fitting Euler vector for all three plate pairs and the Euler vectors derived by the three-plate closure condition suggests the microplate interior is behaving mostly rigidly. Reduced chi-squared values and F-ratio tests support this finding. However, comparison of the predicted motion vectors with the observed structures interpreted to be microplate boundaries indicates that deformation must be occurring over a broad area along the northern microplate boundary. This deformation is suspected to be a direct consequence of the large-scale rift propagation and rapid microplate rotation.

[1]Also at Scripps Institution of Oceanography and now at the University of South Florida, Department of Marine Science, St. Petersburg, Florida 33701

Introduction

The Easter microplate exists along the fastest divergent boundary of the Earth (Fig. 1). It is near the center of a large shallow area characterized by anomalously low surface and shear wave velocities [Woodhouse and Dziewonski, 1984], which together with the pattern of helium isotopes and light rare earth enrichments [Craig et al., 1984; Schilling et al., 1985] indicates very intense mantle convection. Hey et al. [1985] suggest this correlation is unlikely to be coincidental, and that the microplate is probably a transient feature between propagating and failing spreading axes (offset by about 300 km) and may be a modern analog for other large offset spreading axis jumps.

The geometric configuration of this area (Fig. 1) is different from the geometries observed elsewhere for small offset rift jumps as previously noted by Handschumacher et al., [1981]. This is because the southern part of the suspected failing West Rift is propagating southeastward towards the southern part of the northward propagating East Rift. This is different than what is observed at small offset propagating rift systems [e.g., Hey et al., 1986] where failing rifts are situated progressively farther away from the new rift (as one moves in the direction opposite to the propagation direction). The general geometry of the microplate is more like an enlarged overlapping spreading center (OSC) [Macdonald and Fox, 1983; Lonsdale, 1983] except that the microplate rift tips appear to be connected to transform zones.

The microplate was initially suspected to exist because of the ring-like pattern of earthquake epicenters and unusual fault plane mechanisms [Herron, 1972a; Forsyth, 1972]. Engeln and Stein [1984] were the first to investigate the relative plate motions in this area using the magnetic anomaly interpretation of Handschumacher et al. [1981] and slip vectors from the fault plane solutions derived from Forsyth [1972], Anderson et al. [1974] and their own study. Their model was based on 34 data and there were no transform azimuths and only one spreading rate for the Pacific–Easter boundary. Since then, more magnetic, bathymetric and side-scan data have become available. All the new and old magnetic anomaly data have been analyzed to obtain spreading rates during the Brunhes (Table 1). There are twice as many data than before, and there are four transform azimuths and seven spreading rates for the Pacific–Easter boundary. These new data (Table 2) have been inverted to determine the recent (0–0.73 Ma) relative motions for the three plates.

Data

A. Seismic Slip Vectors

Twenty seismic slip vectors were selected from various sources (Table 2). For the motion inversion, the assigned uncertainty for each slip vector azimuth is 20 degrees, except for those given a lower uncertainty